Preparation and Solid-State Structural, Electronic, and Magnetic Properties of the 5-Cyano-1,3-benzene-Bridged Bis(1,2,3,5-dithiadiazolyl) and Bis(1,2,3,5-diselenadiazolyl) [5-CN-1,3-$C_6H_3(CN_2E_2)_2$] (E = S, Se)

A. W. Cordes,[1a] R. C. Haddon,[1b] R. G. Hicks,[1c] D. K. Kennepohl,[1c] R. T. Oakley,*[,1c] T. T. M. Palstra,[1b] L. F. Schneemeyer,[1b] S. R. Scott,[1a] and J. V. Waszczak[1b]

Department of Chemistry and Biochemistry, University of Arkansas, Fayetteville, Arkansas 72701; AT&T Bell Laboratories, Murray Hill, New Jersey 07974; and Guelph Waterloo Centre for Graduate Work in Chemistry, Guelph Campus, Department of Chemistry and Biochemistry, University of Guelph, Guelph, Ontario N1G 2W1, Canada

Received January 6, 1993. Revised Manuscript Received March 22, 1993

The preparation and solid-state characterization of the bifunctional radicals [4,4'-(5-cyanobenzene)-1,3-bis(1,2,3,5-dithiadiazolyl)] and [4,4'-(5-cyanobenzene)-1,3-bis(1,2,3,5-diselenadiazolyl)] [5-CN-1,3-$C_6H_3(CN_2E_2)_2$] (E = S, Se) are described. The crystals of the two title compounds are isomorphous and belong to the monoclinic space group $P2_1/c$, with (for E = S) a = 7.00(2), b = 30.050(6), c = 10.713(8) Å, β = 104.80(10)°, V = 2179(6) Å^3, Z = 8 and (for E = Se) a = 7.124(4), b = 30.50(2), c = 10.874(2) Å, β = 105.46(3)°, V = 2277(2) Å^3, Z = 8. The crystal structures consist of stacks of diradicals running parallel to x; radical dimerization up and down the stack generates a zigzag arrangement, as seen in the related 1,3-phenylene structures. Along the stacking axis the mean intradimer E–E contacts are 3.12 (E = S) and 3.23 Å (E = Se), while the mean interdimer E- - -E distances are 3.89 (E = S) and 3.91 Å (E = Se). Magnetic and conductivity data are presented and discussed in light of extended Hückel band structure calculations.

Introduction

We have recently reported the structural, magnetic and conductivity properties of a variety of dithia- and diselenadiazolyl radicals **1** (E = S, Se). Our interest in these materials, which lies in their potential as low-dimensional molecular conductors,[2] has focused on the design of R groups that, in the solid state, induce the molecular units to adopt stacked structures with strong intra- and interstack interactions. We have demonstrated that stacking of monofunctional radical dimers can be achieved by the use of cyanoaryl[3] or cyanofuryl[4] substituents, but the long range E- - -E (E = S, Se) contacts between and within the dimer stacks are generally weak. Tighter structures, with better conductivity characteristics, can be generated from bifunctional radicals, such as in the α-phase of the 1,3-phenylene bridged systems **2**.[5]

As a continuation of this work, we have prepared and characterized the cyanobenzene bridged diradicals **3**. These materials incorporate the structure-influencing cyano moiety into a bifunctional radical; stacked structures with strong interannular interactions were anticipated. Herein we report the crystal structures and solid state properties

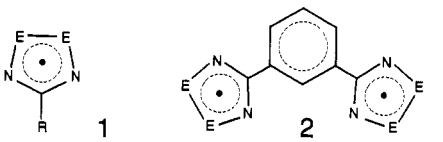

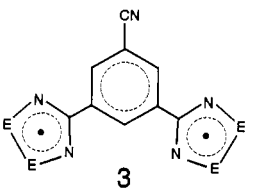

of these two materials. The results are discussed in the light of extended Hückel band structure calculations.

Results and Discussion

Synthesis. The preparative route to **3** (Scheme I) is analogous to that used for other monofunctional and bifunctional radicals.[3-6] The necessary starting material, 5-cyanobenzene-1,3-bis[*N,N,N'*-tris(trimethylsilyl)carboxamidine] (**4**), can be made by treatment of 1,3,5-tricyanobenzene with 2 equiv of lithium bis(trimethylsilyl)-amide, followed by transmetalation with trimethylsilyl chloride. Reaction of the bis(amidine) with 4 mol equiv of SCl_2 or $SeCl_2$ affords, respectively, the bis(1,2,3,5-dithiadiazolium) and bis(1,2,3,5-diselenadiazolium) dication **5** as its dichloride salt. Reduction of the dications with triphenylantimony affords **3** as black powders, which are completely insoluble in all organic media. Both materials

(1) (a) University of Arkansas. (b) AT&T Bell Laboratories. (c) University of Guelph.

(2) Cordes, A. W.; Haddon, R. C.; Oakley, R. T. In *The Chemistry of Inorganic Ring Systems*; Steudel, R., Ed.; Elsevier: Amsterdam, 1992; p 295.

(3) (a) Cordes, A. W.; Haddon, R. C.; Hicks, R. G.; Oakley, R. T.; Palstra, T. T. M. *Inorg. Chem.* **1992**, *31*, 1802.

(4) Cordes, A. W.; Chamchoumis, C. M.; Hicks, R. G.; Oakley, R. T.; Young, K. M.; Haddon, R. C. *Can. J. Chem.* **1992**, *70*, 919.

(5) Andrews, M. P.; Cordes, A. W.; Douglass, D. C.; Fleming, R. M.; Glarum, S. H.; Haddon, R. C.; Marsh, P.; Oakley, R. T.; Palstra, T. T. M.; Schneemeyer, L. F.; Trucks, G. W.; Tycko, R.; Waszczak, J. V.; Young, K. M.; Zimmerman, N. M. *J. Am. Chem. Soc.* **1991**, *113*, 3559.

(6) Del Bel Belluz, P.; Cordes, A. W.; Kristof, E. M.; Kristof, P. V.; Liblong, S. W.; Oakley, R. T. *J. Am. Chem. Soc.* **1989**, *111*, 9276.

0897-4756/93/2805-0820$04.00/0

Scheme I

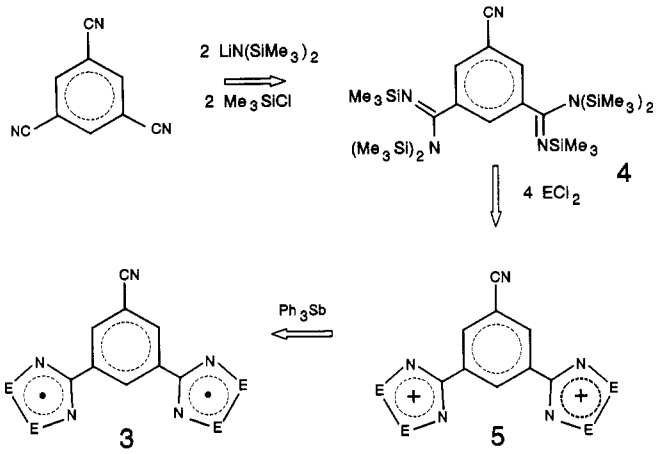

Table I. Non-Hydrogen Positional Parameters and B_{iso} for 3 (E = S) (ESDs Refer to the Last Digit Printed)[a]

	x	*y*	*z*	B_{iso}
S1	0.8617(7)	0.96663(12)	0.6398(4)	3.47(21)
S2	0.9019(7)	0.90038(12)	0.6957(4)	3.50(21)
S3	0.6631(7)	0.71308(13)	0.1983(4)	3.58(21)
S4	0.5984(7)	0.72485(13)	0.0009(4)	3.54(21)
S5	0.4192(7)	0.96156(12)	0.6320(4)	3.91(24)
S6	0.4494(7)	0.89532(12)	0.6891(4)	3.57(22)
S7	0.1155(7)	0.70683(13)	0.2040(4)	3.50(21)
S8	0.0388(7)	0.71742(13)	0.0051(4)	3.36(20)
N1	0.8297(24)	0.9639(5)	−0.0882(13)	4.8(9)
N2	0.8336(21)	0.9556(4)	0.4852(11)	3.8(7)
N3	0.8755(20)	0.8812(4)	0.5486(11)	3.8(7)
N4	0.7054(20)	0.7654(4)	0.2368(11)	3.5(7)
N5	0.6295(19)	0.7787(4)	0.0136(12)	3.1(6)
N6	0.3299(24)	0.9561(5)	−0.0950(13)	5.3(9)
N7	0.3678(20	0.9497(4)	0.4786(11)	3.4(6)
N8	0.4038(20)	0.8758(4)	0.5418(11)	3.5(7)
N9	0.1769(19)	0.7584(4)	0.2407(12)	3.6(7)
N10	0.0892(19)	0.7704(4)	0.0167(11)	3.3(7)
C1	0.7873(25)	0.9141(5)	0.0979(14)	3.3(8)
C2	0.8199(23)	0.9294(5)	0.2244(14)	3.2(7)
C3	0.8055(22)	0.8998(4)	0.3231(14)	2.8(7)
C4	0.7621(21)	0.8560(4)	0.2897(14)	2.7(6)
C5	0.7280(24)	0.8395(5)	0.1625(15)	3.3(8)
C6	0.7466(24)	0.8697(5)	0.0694(14)	3.5(8)
C7	0.8078(24)	0.9431(5)	−0.0033(15)	3.4(8)
C8	0.8387(24)	0.9140(5)	0.4585(14)	3.3(8)
C9	0.6828(25)	0.7932(5)	0.1365(15)	3.4(8)
C10	0.2838(24)	0.9047(5)	0.0880(14)	3.2(7)
C11	0.3253(24)	0.9208(5)	0.2141(15)	3.5(8)
C12	0.3149(23)	0.8925(5)	0.3151(14)	2.9(8)
C13	0.2653(23)	0.8490(5)	0.2855(14)	3.2(8)
C14	0.2165(24)	0.8321(5)	0.1586(14)	3.3(8)
C15	0.2305(23)	0.8600(5)	0.0615(13)	3.3(8)
C16	0.3039(24)	0.9339(5)	−0.0140(4)	3.3(8)
C17	0.3607(24)	0.9068(5)	0.4511(14)	3.3(8)
C18	0.1571(24)	0.7856(5)	0.1373(15)	3.3(8)
H4	0.755	0.836	0.356	3.3
H2	0.854	0.960	0.244	3.8
H6	0.734	0.860	−0.016	4.1
H13	0.264	0.829	0.354	3.8
H11	0.363	0.951	0.230	4.0
H15	0.206	0.849	−0.025	3.9

[a] B_{iso} is the mean of the principal axes of the thermal ellipsoid.

can, however, be purified by high-vacuum sublimation at 220 °C/10^{-2} Torr (E = S) or 250 °C/10^{-2} Torr (E = Se).

Crystal Structures. Crystals of **3** (E = S, Se) are isomorphous, and belong to the monoclinic space group $P2_1/c$; non-hydrogen atom coordinates are provided in Tables I and II; all internal bond lengths and angles are normal (see summary in Table III). An ORTEP drawing of the asymmetric unit (for E = S), giving the atom-numbering scheme, is shown in Figure 1.

Table II. Non-Hydrogen Positional Parameters and B_{iso} for 3 (E = Se) (ESDs Refer to the Last Digit Printed)[a]

	x	*y*	*z*	B_{iso}
Se1	0.8273(3)	0.97199(6)	0.65761(14)	2.72(8)
Se2	0.8784(3)	0.89942(6)	0.72170(13)	2.81(8)
Se3	0.6429(3)	0.71136(6)	0.23338(15)	3.10(8)
Se4	0.5651(3)	0.72289(6)	0.01475(15)	3.05(8)
Se5	0.3699(3)	0.96528(6)	0.64316(14)	2.84(8)
Se6	0.4166(3)	0.89259(6)	0.70740(14)	2.88(8)
Se7	0.1044(3)	0.70462(6)	0.23682(15)	3.03(8)
Se8	0.0092(3)	0.71393(6)	0.01658(14)	2.86(8)
N1	0.8272(24)	0.9619(5)	−0.0629(12)	3.5(7)
N2	0.7940(20)	0.9562(5)	0.4951(11)	2.6(6)
N3	0.8474(22)	0.8825(5)	0.5615(11)	2.7(6)
N4	0.6914(23)	0.7683(5)	0.2638(11)	3.1(7)
N5	0.6041(20)	0.7807(5)	0.0381(11)	2.6(6)
N6	0.3341(25)	0.9508(5)	−0.0784(12)	3.8(8)
N7	0.3254(20)	0.9492(4)	0.4778(10)	2.4(6)
N8	0.3827(21)	0.8746(4)	0.5464(11)	2.7(6)
N9	0.1645(21)	0.7596(4)	0.2607(12)	2.7(3)
N10	0.0732(21)	0.7710(5)	0.0353(11)	2.7(6)
C1	0.7825(23)	0.9119(5)	0.1196(13)	1.9(3)
C2	0.8142(24)	0.9285(5)	0.2441(14)	2.2(3)
C3	0.7859(23)	0.8995(4)	0.3389(13)	1.8(3)
C4	0.7348(24)	0.8567(5)	0.3082(14)	2.2(3)
C5	0.7081(23)	0.8399(4)	0.1833(13)	1.9(3)
C6	0.7352(24)	0.8694(5)	0.0906(14)	2.4(3)
C7	0.8132(25)	0.9415(5)	0.0199(14)	2.4(3)
C8	0.8072(24)	0.9153(5)	0.4746(13)	2.0(3)
C9	0.6640(25)	0.7941(5)	0.1604(14)	2.3(3)
C10	0.2685(25)	0.9016(5)	0.1015(14)	2.4(3)
C11	0.3118(25)	0.9189(5)	0.2255(14)	2.4(3)
C12	0.2899(24)	0.8905(4)	0.3242(14)	2.0(3)
C13	0.2371(24)	0.8486(5)	0.2983(13)	2.0(3)
C14	0.1940(24)	0.8311(5)	0.1736(13)	2.0(3)
C15	0.2173(25)	0.8590(5)	0.0762(14)	2.6(3)
C16	0.305(3)	0.9294(5)	−0.0012(15)	2.7(3)
C17	0.3348(24)	0.9074(4)	0.4590(13)	1.9(3)
C18	0.137(3)	0.7855(5)	0.1555(15)	2.6(3)
H2	0.851	0.958	0.262	3.0
H4	0.711	0.837	0.371	3.0
H6	0.723	0.861	0.005	3.2
H11	0.357	0.948	0.242	3.2
H13	0.225	0.830	0.365	2.8
H15	0.192	0.848	−0.009	3.3

[a] B_{iso} is the mean of the principal axes of the thermal ellipsoid.

Table III. Summary of Intra- and Intermolecular Distances (Å)

	E = S	E = Se
mean E–E (range)	2.079(8)	2.322(6)
mean E–N (range)	1.64(2)	1.78(8)
mean C–N (range)	1.33(7)	1.34(9)
Intrastack Contacts		
d_1 E1- - -E5	3.081(11)	3.227(3)
d_2 E2- - -E6	3.154(11)	3.258(3)
d_3 E3- - -E7 at ***a***	3.158(11)	3.284(3)
d_4 E4- - -E8 at ***a***	3.080(11)	3.170(3)
d_5 E1- - -E5 at ***a***	3.928(13)	3.916(4)
d_6 E2- - -E6 at ***a***	3.854(13)	3.884(3)
d_7 E3- - -E7	3.853(13)	3.852(4)
d_8 E4- - -E8	3.935(13)	3.976(4)
Interstack Contacts[a]		
B/B E1- - -E5 at ***b***	3.752(7)	3.726(3)
A/B E2- - -E7 at ***d***	3.543(6)	3.542(3)
A/B E2- - -E3 at ***c***	3.800(6)	3.789(3)
A/B E6- - -E3 at ***c***	3.575(6)	3.534(3)
A/B E6- - -E7 at ***c***	3.886(7)	3.771(3)
A/A E4- - -E3 at ***e***	3.866(6)	3.820(3)

A = $1 + x, y, z$ **b** = $1 - x, 2 - y, z$
c = $x, 1^1/_2 - y, {}^1/_2 + z$ **d** = $1 + x, 1^1/_2 - y, {}^1/_2 + z$
e = $x, 1^1/_2 - y, -{}^1/_2 + z$

[a] A and B refer to the rings indicated in Figure 3.

The crystal structures consist of stacks of diradicals running parallel to the *x* axis. As in the cyanoaryl and

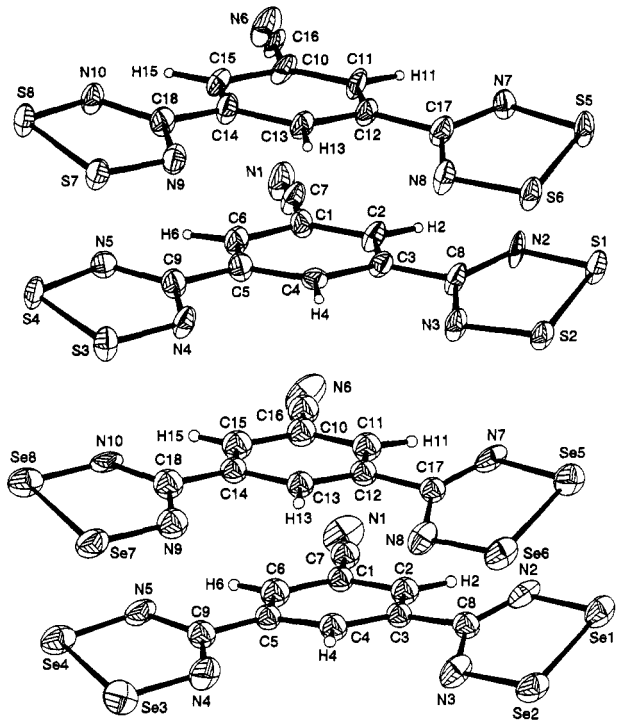

Figure 1. ORTEP drawings of the asymmetric units in **3**, showing atom numbering. E = S (above) and E = Se (below).

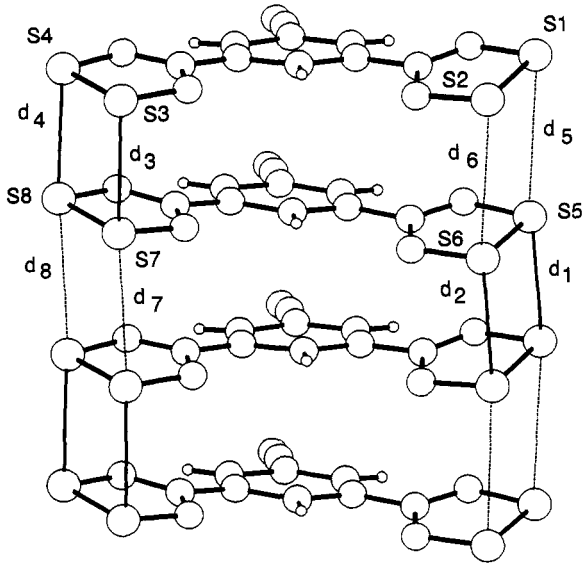

Figure 2. Zigzag stacking of molecular units in **3** (E = S) along the *x* direction.

cyanofuryl structures reported earlier, these materials also are characterized by CN- - -E contacts (mean value 3.10/3.12 Å for E = S/Se) which facilitate the orientation of the molecular plates in a coplanar arrangement.[7] Figure 2 shows a single stack of diradicals, and illustrates the zigzag dimerization motif reminiscent of that observed earlier for the α-phase of the 1,3-phenylene bridged diradicals **2**. Within each stack the mean intradimer contacts (3.12/3.23 Å for S/Se) are comparable to those found for α-**2** (3.14/3.28 Å for S/Se). The mean interdimer contacts (3.89/3.91 Å for S/Se) are also similar to, although

(7) Similar effects have been observed elsewhere. (a) Suzuki, T.; Fukui, H.; Yamashita, Y.; Kabuto; C.; Tanaka, S.; Harasawa, M.; Mukui, T.; Miyashi, T. *J. Am. Chem. Soc.* **1992**, *118*, 3034. (b) Alcock, N. W. *Adv. Inorg. Radiochem.* **1972**, *15*, 1.

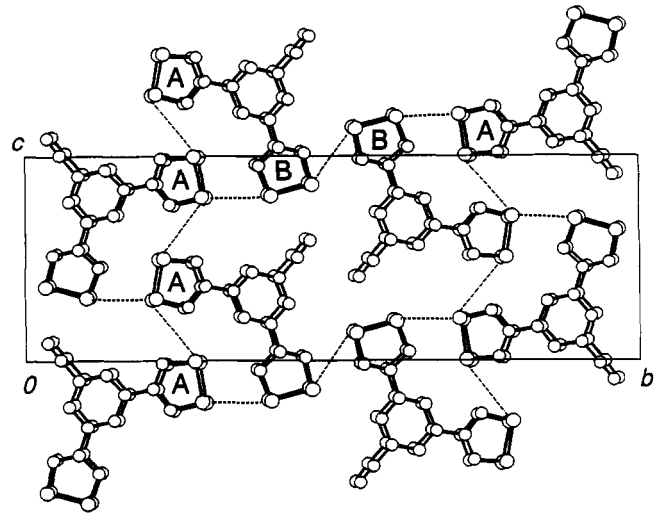

Figure 3. Packing of **3** (E = S), viewed parallel to *x*.

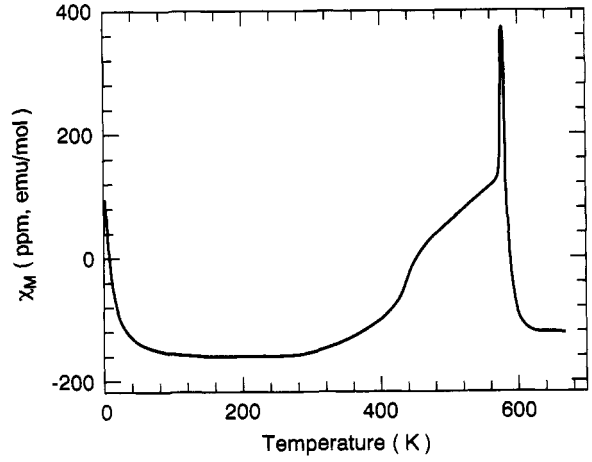

Figure 4. Magnetic susceptibility of **3** (E = S) as a function of temperature.

fractionally shorter than, those seen in α-**2** (3.97/4.014 Å for S/Se). Despite the rocking of the molecular plates about the stacking axis, the centroid-to-centroid distances for the benzene rings remains quite constant, i.e., 3.51/3.52 Å for E = S and 3.58/3.57 Å for E = Se (cf. 3.54/3.58 Å and 3.60/3.69 Å for S/Se in α-**2**).

Figure 3 illustrates the crystal packing viewed parallel to the columnar stacking direction. The packing arrangement affords a range of short interstack E- - -E interactions, defined (in Table III) in terms of the two symmetry distinct A and B columns. Interdimer interactions parallel to *z* are continuous (i.e., contacts along *z* between type A columns form an infinite sequence), while those running in the *y* direction are restricted to four-column groups (i.e., A/B/B/A). The view of the packing provided in Figure 3 also illustrates the oblique (rather than the more typical head-on) CN- - -E contacts that help generate the sheetlike arrays of molecular units.

Magnetic and Conductivity Measurements. The measured magnetic susceptibility of **3** as a function of temperature is shown in Figures 4 and 5. As observed in **2** the low-temperature regime shows Curie behavior, consistent with the presence of low levels of paramagnetic defects arising from unpaired radicals. The concentration of defects obtained from a Curie–Weiss fit to the data in Figures 4 and 5 was 0.34% (E = S) and 1.14% (E = Se) on a per molecule basis, which is similar to the values

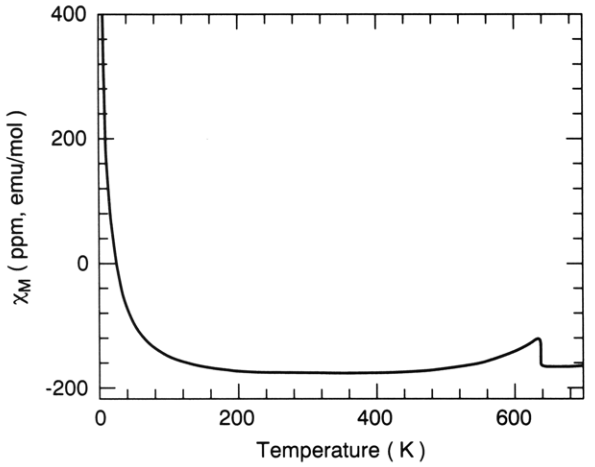

Figure 5. Magnetic susceptibility of **3** (E = Se) as a function of temperature.

found for **2** (0.97% for E = S and 0.51% for E = Se). The θ value was −3 (E = S) and 3 (E = Se) K and the measured diamagnetism −163 (E = S) and −178 (E = Se) ppm emu mol^{-1}. The high-temperature behavior of the magnetic susceptibilities of **2** and **3** (E = S) are quite similar. Both compounds show a large enhancement in the paramagnetism above room temperature which continues to increase up until the decomposition temperature. Just before the steep rise in susceptibility which precedes decomposition, the enhancement in the paramagnetism of both compounds amounts to about 300 emu ppm mol^{-1}, which corresponds to about 0.5 spins per molecule on a Curie basis.[5] The origin of the enhanced paramagnetism in **2** (E = S) was previously ascribed, on the basis of ESR and NMR measurements, to the presence of thermally generated phase kinks in the lattice.[5,8]

The temperature dependence of the magnetic susceptibilities of **2** and **3** (E = Se) are quite similar; in contrast to their sulfur counterparts the increase in susceptibility at elevated temperatures (below the decomposition point) is minimal. On the basis of the behavior of the sulfur compounds, in which there is no significant conductivity enhancement associated with the high-temperature phase kinks, we attribute the observed conductivity of the selenium compounds to thermally activated electrons.[5,9] The conductivity of **3** (E = Se), measured along the needle axis, is shown Figure 6. The temperature dependence of the conductivity gives an activation energy of 0.64 eV, and the conductivity at 300 K is less than 10^{-7} S cm^{-1}. The conductivity of **2** (E = Se) was found to be greater than 10^{-4} S cm^{-1} at 300 K with an activation energy of 0.55 eV. The difference in the conductivities of **2** and **3** (E = Se), as discussed below, seems to stem from the more well developed 3-dimensionality in the former.

Band Structure Calculations. Extended Hückel band structure calculations, employing the parameters described previously,[10] have been performed on structures related to the full 3-dimensional structures of **3** (E = S, Se). As we noted in an earlier paper on the band structures of cyanoaryl-substituted radicals, and as a result of the

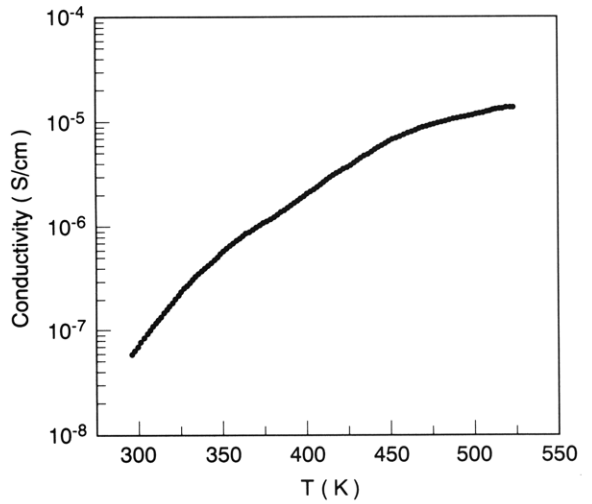

Figure 6. Single crystal conductivity of **3** (E = Se) as a function of temperature.

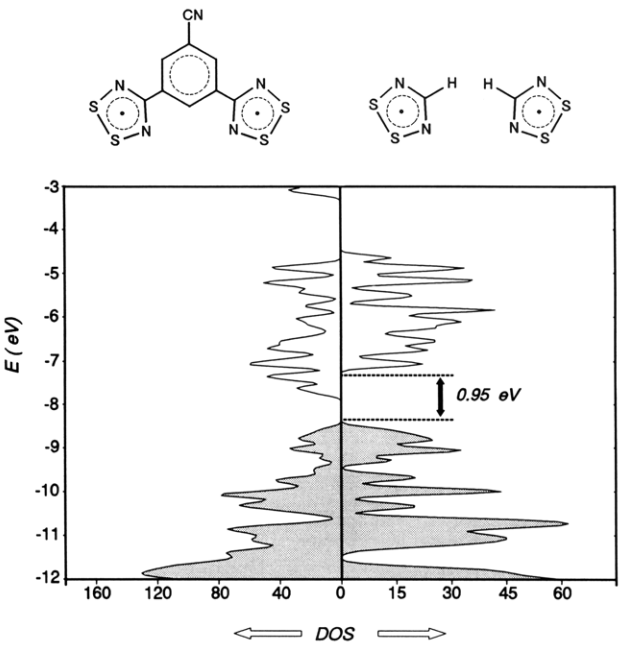

Figure 7. Density of states (DOS, eV per cell) for **3** (E = S). Full structure (LHS) and H substituent only (RHS).

approximations inherent in the theoretical method used, the low-lying π^*-acceptor levels of cyano groups collectively intrude into the valence-conduction bandgap associated with the interacting radical centers.[11] To that end we have performed two sets of calculations, one based on the complete structure, and the other based upon a model in which the "organic" ligands have been replaced by a simple H substituent; the latter calculations then refer to the interactions of HCN_2E_2 rings located in the lattice positions of **3**. The results are presented in Figures 7–9, which illustrate the density of states (DOS) and dispersion curves for the valence and conduction bands. The density of states diagrams for the full structures show, as before, the low-lying intruder states in the bandgap region. Replacement of the organic ligand by an H atom provides a more realistic estimate of the bandgap.

The density of states data obtained from the simplified (H only) structures indicate that the compounds are

(8) Allen, L. C.; Warren, W. W.; Haddon, R. C.; Oakley, R. T.; Cordes, A. W. *Phys. Rev. B* **1991**, *43*, 11456.
(9) Cordes, A. W.; Haddon, R. C.; Hicks, R. G.; Oakley, R. T.; Palstra, T. T. M.; Schneemeyer, L. F.; Waszczak, J. V. *J. Am. Chem. Soc.* **1992**, *114*, 1729.
(10) Cordes, A. W.; Haddon, R. C.; Oakley, R. T.; Schneemeyer, L. F.; Waszczak, J. V.; Young, K. M.; Zimmerman, N. M. *J. Am. Chem. Soc.* **1991**, *113*, 582.
(11) Davis, W. M.; Hicks, R. G.; Oakley, R. T.; Zhao, B.; Taylor, N. J. *Can. J. Chem.* **1993**, *71*, 180.

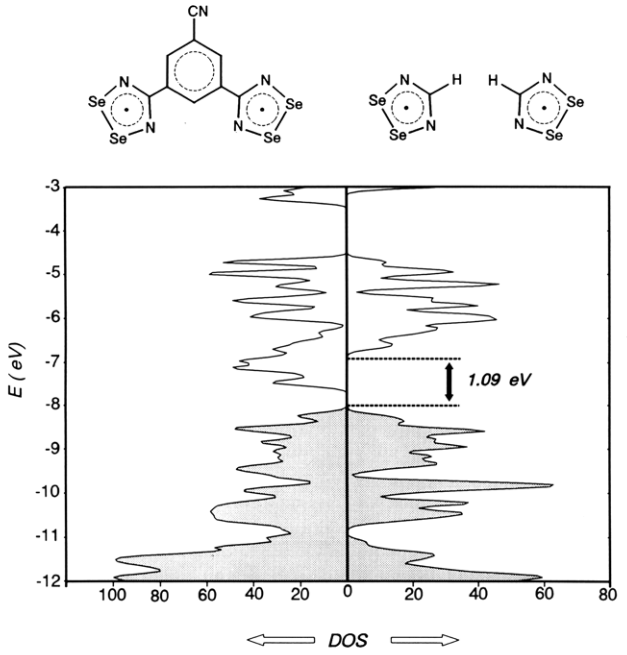

Figure 8. Density of states (DOS, eV per cell) for **3** (E = Se). Full structure (LHS) and H substituent only (RHS).

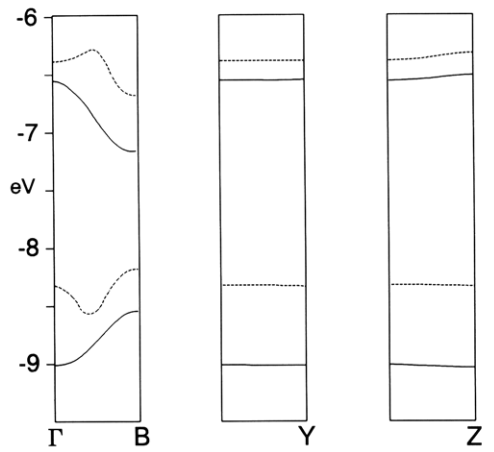

Figure 9. Dispersion of highest valence (lower) and lowest conduction (upper) bands of **3** (model structure with cyanoaryl group replaced by H) along the principal directions of reciprocal space, where Γ = (0, 0, 0,), B = (a^*/2, 0,0), Y = (0, b^*/2, 0), Z = (0, 0, c^*/2). Solid lines are E = S, dashed lines are E = Se.

semiconductors, with calculated bandgaps of 0.95/1.06 eV (E = S/Se). These values are greater than those found in **2**, even though the latter calculations were performed on partial rather than full structures, i.e., on four-column clusters about the 4_1 and $\bar{4}$ axes; the calculated bandgaps for these two models were 0.96/0.78 eV (for S/Se) and 1.12/0.84 eV (for S/Se). In the latter systems, lateral E- - -E interactions between the radicals within the pinwheel clusters were quite effective in increasing the band dispersion. In the present case, lateral interactions appear to have little effect. Even though both the number and magnitude of the intercolumnar interactions listed in Table III suggest otherwise, the dispersion relations illustrated in Figure 9 indicate that the structures are highly one-dimensional; presumably the directional properties of these contacts are not conducive to effective overlap. Dispersion along a^*, which in this monoclinic cell approximates the stacking direction in real space, is substantial in both the valence and conduction bands and is quite comparable in magnitude to that which is found along the stacking axis in subunits of **2**. However, there is virtually no dispersion along b^*, which loosely corresponds to interactions parallel to b. This finding is consistent with the fact that there is no continuous network of E- - -E contacts in this direction (*vide supra*). In keeping with the extended contacts between the type A radical centers, there is more dispersion along c^*, although here also the extent is minimal.

Experimental Section

Starting Materials and General Procedures. 1,3,5-Benzenetricarbonyl trichloride, lithium bis(trimethylsilyl)amide, sulfur dichloride, trimethylsilyl chloride, and triphenylantimony were all obtained commercially (Aldrich). Sulfur dichloride was distilled before use, and $LiN(SiMe_3)_2$ was converted into its diethyl etherate in order to facilitate amidine synthesis.[12] Selenium tetrachloride was prepared using the literature method.[13] Acetonitrile (Fisher HPLC grade) was purified by distillation from P_2O_5. 1,3,5-Tricyanobenzene was prepared by standard literature methods.[14] All reactions were performed under an atmosphere of nitrogen. ^{1}H NMR spectra were recorded at 200 MHz on a Varian Gemini 200 spectrometer. Infrared spectra (CsI optics, Nujol mulls) were obtained on a Nicolet 20SX/C FTIR instrument. Elemental analyses were performed by MHW Laboratories, Phoenix, AZ.

Preparation of 5-Cyanobenzene-1,3-bis[*N,N,N'*-tris(trimethylsilyl)carboxamidine] (4). $LiN(SiMe_3)_2{\cdot}Et_2O$ (20.7 g, 0.86 mmol) was added, as a dry solid, to a slurry of 1,3,5-tricyanobenzene (6.6 g, 43 mmol) in 150 mL of toluene, and the mixture heated at gentle reflux overnight. Excess trimethylsilyl chloride (15 mL) was added, and the mixture heated at reflux for a further 16 h. The mixture was then filtered to remove LiCl, and the filtrate concentrated to about half its original volume. Upon cooling to room temperature, a white precipitate of 5-cyanobenzene-1,3-benzenebis[*N,N,N'*-tris(trimethylsilyl)carboxamidine] (**4**) was formed. The crude product was collected by filtration, washed with CH_3CN, and dried in vacuo. Recrystallization from toluene/CH_3CN (2:1) afforded colorless crystals (10.5 g, yield 40%), mp 140–42 °C, ^{1}H NMR (δ, $CDCl_3$) 0.091 (Me_3Si, 54H), 7.68 (t, aromatic, 1H, J = 1.9 Hz), 7.60 (d, aromatic, 2H, J = 1.9 Hz). Anal. Calcd for $C_{27}H_{57}N_5Si_6$: C, 52.28; H, 9.26; N, 11.29. Found: C, 52.29; H, 9.06; N, 11.25.

Preparation of [5-CN-1,3-$C_6H_3(CN_2S_2)_2$] (3, E = S). Excess (2 mL) sulfur dichloride in 10 mL of CH_3CN was added to a slurry of **4** (3.1 g, 5 mmol) in 100 mL of CH_3CN, and the resulting orange slurry heated at reflux for 16 h. The crude bis(dithiadiazolium) salt **5** so produced was flitered, washed with CH_3CN, and pumped dry in vacuo. This dichloride salt was reduced by treatment with excess Ph_3Sb (1.9 g, 5.4 mmol) in refluxing CH_3CN for 48 h. The black precipitate of crude bis(1,2,3,5-dithiadiazolyl) [5-CN-1,3-$C_6H_3(CN_2S_2)_2$] (**3**) was filtered off, dried in vacuo, and purified by sublimation at 220 °C/10^{-2} Torr as small flat needles (400 mg, check yield 26%), dec >335 °C. Larger crystals suitable for X-ray work were obtained by sealed tube sublimation at 250 °C. The material is completely insoluble in all organic media. Anal. Calcd for $C_9H_3N_5S_4$: C, 34.94; H, 0.98; N, 22.64. Found: C, 35.0; H, 1.14; N, 22.77. IR 2240 (νCN) and (1600–250 cm^{-1}) 1338 (vs), 1268 (m), 1125 (w), 1000 (w), 990 (m), 897 (m), 837 (w), 820 (m), 777 (s), 767 (s), 689 (m), 580 (m), 507 (s) cm^{-1}.

Preparation of [5-CN-1,3-$C_6H_3(CN_2Se_2)_2$] (3, E = Se). Solid **4** (3.1 g, 5 mmol) was added to a solution of $SeCl_2$ prepared *in situ* from Se (0.78 g, 10 mmol) and $SeCl_4$ (2.2 g, 10 mmol) in 100 mL of CH_3CN, and the resulting dark red slurry heated at reflux for 16 h. The crude bis(diselenadiazolium) salt **5** so produced was filtered, washed with CH_3CN, and pumped dry in vacuo. This dichloride salt was reduced by treatment with excess Ph_3Sb

(12) Boeré, R. T.; Oakley, R. T.; Reed, R. W. *J. Organomet. Chem.* **1987**, *331*, 161.
(13) Brauer, G. *Handbook of Preparative Chemistry*; Academic: New York, 1963; Vol. 1, p 423.
(14) Bailey, A. S.; Henn, B. R.; Langdon, J. M. *Tetrahedron* **1963**, *19*, 161.

Table IV. Crystal Data for 3 (E = S, Se)

	$S_4N_5C_9H_3$	$Se_4N_5C_9H_3$
fw	309.40	497.00
a, Å	7.00(2)	7.124(4)
b, Å	30.050(6)	30.50(2)
c, Å	10.713(8)	10.874(2)
β, deg	104.80(10)	105.46(3)
V, Å^3	2179(6)	2277(2)
d(calcd), g cm^{-3}	1.887	2.889
space group	$P2_1/c$	$P2_1/c$
Z	8	8
λ, Å	0.710 73	0.710 73
temp, K	296	296
μ, mm^{-1}	7.82	15.83
$R(F^2)$, $R_w(F^2)$[a]	0.126, 0.156	0.71, 0.94

[a] $R = [\Sigma||F_o| - |F_c||]/[\Sigma|F_o|]$; $R_w = \{[\Sigma w||F_o| - |F_c||^2]/[\Sigma(w|F_o|^2)]\}^{1/2}$.

(1.85 g, 5.2 mmol) in refluxing CH_3CN for 48 h. The black precipitate of crude bis(1,2,3,5-diselenadiazolyl) [5-CN-1,3-C_6H_3-$(CN_2S_2)_2$] (**3**) was filtered off, dried in vacuo, and purified by sublimation at 250 °C/10^{-2} Torr as small bronze needles (400 mg, yield 26%), dec >350 °C. Larger crystals suitable for X-ray work were obtained by sealed tube sublimation at 270 °C. The material is completely insoluble in all organic media. Anal. Calcd for $C_9H_3N_5Se_4$: C, 21.75; H, 0.61; N, 14.09. Found: C, 21.60; H, 0.76; N, 14.18. IR: 2227 (ν(CN) and (1600–250 cm^{-1}) 1315 (m), 1299 (w), 1274 (s), 963 (m), 937 (w), 890 (m), 752 (m), 732 (s), 691 (m), 615 (m), 590 (w), 573 (w), 475 (w), 445 (w), 403 (w), 382 (s) 321 (w) 281 (w) cm^{-1}.

X-ray Measurements. X-ray data were collected on a Rigaku AFC5R with monochromated Cu Kα radiation and using a 12-kW rotating anode generator. Data were collected using an ω–2θ technique, and the structures were solved by direct methods and refined by full-matrix least squares techniques which minimized $\Sigma w(\Delta F)^2$. No extinction corrections were made. A summary of crystallographic data is provided in Table IV. Crystals of both compounds suffered severely from twinning, which led to elevated R factors, especially for the sulfur compound. Lateral disorder between columns along the stacking axis was treated by the inclusion of disorder atoms. For the sulfur compound 10 partial S peaks were located in difference maps. Their positions were frozen and isotropic U values set at 0.04; only their occupation parameters were allowed to vary. The resulting occupancy factors for these disorder ranged from 0.06 to 0.09. In the selenium compound 12 partial Se peaks were located in difference maps. Their positions were frozen and isotropic U values set at 0.04; only their occupation parameters were allowed to vary. The resulting occupancy factors for these disorder atoms ranged from 0.03 to 0.06.

Magnetic Measurements. The magnetic susceptibility was measured from 4.2 to about 650 K by using the Faraday technique. Details of the apparatus have been previously described.[15]

Conductivity Measurements. Single-crystal measurements were made along the long (a) axis of the crystals, using silver–epoxy to attach the leads. Four point measurements were made in an argon atmosphere, using a Keithley 236.

Band Structure Calculations. The band structure calculations were carried out with the EHMACC suite of programs using the parameters discussed previously.[10,16] The off-diagonal elements of the Hamiltonian matrix were calculated with the standard weighting formula.[17]

Acknowledgment. Financial support at Guelph was provided by the Natural Sciences and Engineering Research Council of Canada and at Arkansas by the National Science Foundation (EPSCOR program).

Supplementary Material Available: Tables of crystal data, structure solution and refinement (S1), full positional parameters (including disordered atoms) (S2, S3), distances and angles (S4, S5), and anisotropic thermal parameters (S6, S7) for the title compounds **3** (E = S, Se) (8 pages). Ordering information is given on any current masthead page.

(15) (a) DiSalvo, F. J.; Waszczak, J. V. *Phys. Rev.* **1981**, *B23*, 457. (b) DiSalvo, F. J.; Waszczak, J. V.; Tauc, J. *Phys. Rev.* **1972**, *B6*, 4574.
(16) Basch, H.; Viste, A.; Gray, H. B. *Theor. Chim. Acta* **1965**, *3*, 458.
(17) Ammeter, J. H.; Burghi, H. B.; Thibeault, J. C.; Hoffmann, R. *J. Am. Chem. Soc.* **1978**, *100*, 3686.